ioMosaic®
Minimizing risk. Maximizing potential.®

Two-phase Flow Onset and Disengagement Methods

An ioMosaic® Publication

G. A. Melhem, Ph.D., FAIChE

This page is intentionally left empty

IOMOSAIC® CORPORATION

Two-phase Flow Onset and Disengagement Methods

Process Safety and Risk Management Practices

authored by

G. A. Melhem, Ph.D., FAIChE

Printed April 15, 2025

This page is intentionally left empty

Notice:

This document was prepared by ioMosaic® Corporation (**ioMosaic**) for Public Release. This document represents ioMosaic's best judgment in light of information available and researched prior to the time of publication.

Opinions in this document are based in part upon data and information available in the open literature, data developed or measured by ioMosaic, and/or information obtained from ioMosaic's advisors and affiliates. The reader is advised that ioMosaic has not independently verified all the data or the information contained therein. This document must be read in its entirety. The reader understands that no assurances can be made that all liabilities have been identified. This document does not constitute a legal opinion.

No person has been authorized by ioMosaic to provide any information or make any representation not contained in this document. Any use the reader makes of this document, or any reliance upon or decisions to be made based upon this document are the responsibility of the reader. ioMosaic does not accept any responsibility for damages, if any, suffered by the reader based upon this document.

Revision Log:

Revision 1: November 9, 2020
Revision 2: December 7, 2024
Revision 3: January 2, 2025

...

Table of Contents

List of Figures

List of Tables

1 Introduction

Two-phase flow is often considered in system hydraulics as well as the evaluation and design of pressure relief and effluent handling systems. A variety of scenarios can lead to two-phase flow under relief conditions.

In general, two-phase flow during relief can occur because of flow hydrodynamics and poor vapor/liquid disengagement where (a) the liquid swells due to generation of vapor bubbles in the liquid [1], (b) fluid expansion occurs due to heating, and/or (c) the superficial vapor velocity is high enough through the pressure relief device. Oversized relief devices can induce two-phase flow because a large relief flow area yields a higher superficial vapor velocity. Runaway chemical reactions and/or chemical systems that are viscous and/or foamy [1] almost always lead to homogeneous two-phase flow.

Two-phase flow can also occur by entrainment, for example, where gas is sparged at a high enough rate in the liquid. In some systems, condensation leading to two-phase flow in the discharge piping can also occur due to expansion cooling caused by pressure reduction through a control valve or a pressure relief device.

Numerous two-phase flow models have appeared in the literature. These models represent broad ranges of theory. Some are based on single-phase critical flow, others on homogeneous equilibrium flow, frozen flow, separated flow, slip flow, and/or non-equilibrium flow.

Homogeneous equilibrium flow models assume equal vapor and liquid velocities and calculate the change of quality with pressure using an isenthalpic or isentropic thermodynamic path. Homogeneous frozen models assume equal vapor and liquid flow velocities and that the quality is frozen along the flow path, i.e., no change with respect to pressure or temperature. The separated flow models assume different vapor and liquid flow velocities and account for mass, momentum and heat transfer between the separate phases.

2 Two-phase Flow Implications

It is preferred to eliminate or significantly reduce the potential for two-phase flow. This can be accomplished by either (a) reducing the risk/likelihood of the scenarios that can lead to two-phase flow to a tolerable level and/or (b) specific relief and effluent handling systems design considerations and implementations [2].

More mass is vented from a vessel during two-phase flow than during all vapor flow. During all vapor flow, the liquid has to make up the lost vapor and beneficial energy tempering occurs. This helps to reduce the relief requirements for fire exposure scenarios for example.

As a result of more mass being discharged due to two-phase flow, potential dispersion, fire, and explosion hazard footprints can become significantly larger. Vent containment and/or flow separa-

[1] Generation of bubbles can occur due to mechanical means and/or chemical reactions including decomposition reactions.

[2] This includes the use of quenching systems that suppress chemical reactions that can cause two-phase flow, such as the introduction of a quench fluid, and/or the quick injection of an inhibitor or a neutralizing agent.

tion are often required to reduce the risks of two-phase flow. When homogeneous two-phase flow occurs, the specific ratio of vapor to liquid does not change in the vessel during venting and as result beneficial energy tempering does not occur. When more vapor is vented relative to liquid, beneficial energy tempering occurs because the liquid has to make up the lost vapor. This is one of the primary reasons why homogeneous two-phase flow results in large relief requirements for vessels exposed to external fire, external or internal heating, and/or where chemical runaway reactions are the cause of the homogeneous two-phase flow.

It is therefore important to be able to determine:

(a) what configurations and/or process conditions can lead to two-phase flow,

(b) the vapor quality entering the vent, and

(c) the rate at which two-phase flow occurs.

Undoubtedly, one of the most important contributions of the American Institute of Chemical Engineers (AIChE) design institute of emergency relief systems (DIERS) to chemical process safety is the development of the coupling equation which can be used to determine if and when two-phase will occur and what the vapor quality entering the vent will be. DIERS also published methods for the estimation of two-phase flow rates.

3 Two-phase Flow Patterns

The treatment of two-phase flow is complex by nature because a sequence of flow patterns can develop within a given process pipe or unit. Figure 1 shows typical two-phase flow patterns occurring in horizontal and vertical piping configurations.

Stratified Gas [3] and liquid are separated in two cocurrently flowing phases, with liquid flowing as a layer along the channel bottom.

Wavy Stratified flow where flow instabilities cause a wavy gas-liquid interface excluding low flow rates conditions.

Slug Liquid waves tend to bridge the gap between the liquid surface and the channel top, causing the gas phase to move as a slug.

Plug Gas bubbles tend to agglomerate and nearly fill the cross section of the channel, moving as asymmetrical bullet shaped entities.

Bubbly The gas tend to distribute as discrete bubbles in the continuous liquid phase, with bubbles rising towards the top of the channel. A good example is soapy water or bubbly beer.

Churn Similar to bubble flow where the liquid phase is continuous. Typifies clean water or uncontaminated refrigerants where extensive bubble coalescence occurs.

[3] Gas and/or vapor may be used interchangeably in this paper

Figure 1: Approximate two-phase flow patterns

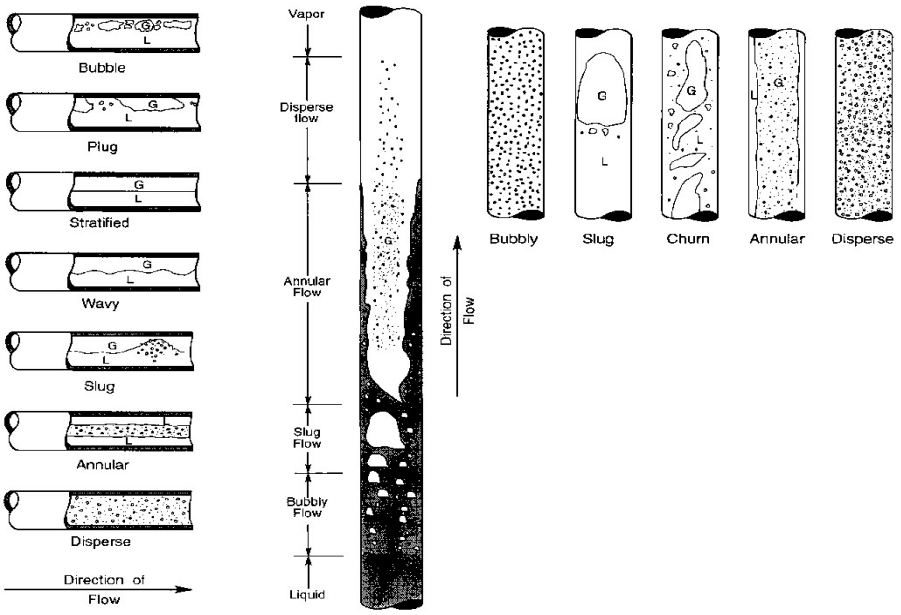

Droplet The vapor forms a continuous phase where the vapor superficial velocity exceeds the liquid entrainment velocity.

Annular At high flow rates the liquid climbs the walls of the channel, forming a ring of nonuniform thickness around a central core of gas. The gas-liquid interface is highly irregular and waves tend to break off, giving rise to dispersed annular flow. At sufficiently high gas flow rates the flow becomes dispersed, during which liquid droplets are distributed in the continuous gas phase.

4 Liquid Full Conditions Due to Thermal Expansion

Two-phase flow can occur due to liquid thermal expansion. This is possible when the initial liquid level at normal storage, transport, or processing conditions is high enough to cause liquid full conditions under external heating, runaway reaction heating, and/or fire exposure. Liquid fill levels are typically maximized during transport where rail cars or storage tanks on ships are used to transport liquids or cryogenic materials. However, the initial liquid fill level should not exceed a maximum limit (see Equation 1) if liquid thermal expansion is a credible scenario.

It is therefore recommended that the initial liquid fill level at normal fill conditions should not exceed 95 % of a liquid full condition at the opening pressure of a reclosing pressure relief device if external heating and/or internal heating is credible:

$$H_{l,\max} \simeq 0.95 \times \frac{\rho_{l,\text{sat}}}{\rho_{l,o}} \tag{1}$$

where $H_{l,\max}$ is the maximum permissible liquid level at the initial normal filling conditions, $\rho_{l,\text{sat}}$ is the saturated liquid density at the opening pressure of the reclosing pressure relief device, and $\rho_{l,o}$ is the liquid density at the initial normal filling conditions.

For example, a wide variety of chemicals are shipped by rail transport including flammable liquids, flammable liquefied gases, reactive monomers, etc. Normal liquid fill levels at ambient conditions can be as high as 95 % in order to maximize the use of the rail car. These high initial liquid levels can cause liquid full conditions when the rail cars are exposed to external heating from a fire for a long enough duration.

Liquid full or near liquid full conditions can cause two-phase flow. For liquids that are initially subcooled and where the rail car has not reached liquid full conditions, liquid thermal expansion causes the vapor space to be compressed and cycling of any installed pressure relief valves. Pressure relief valves on rail cars have not historically been sized for multiphase flow and/or for runaway reactions. Under prolonged external heating, the rail car can become liquid full and intermittent venting of subcooled liquid can occur until the bulk liquid temperature reaches the saturation temperature. This intermittent liquid venting is typically followed by sustained two-phase flow and eventually all vapor flow after vapor/liquid disengagement.

Liquid full conditions can be highly hazardous if pressure relief is not possible because of a damaged or plugged pressure relief valve in a derailment. Under liquid full conditions, every degree of temperature change can result in large pressure increases depending on the isothermal liquid compressibility and liquid properties. For a rail car without pressure relief, pressure increases under liquid full conditions can be significant enough to cause failure of the rail car even with a relatively small increase in temperature.

Table 1 illustrates the maximum liquid fill level at normal fill conditions that will lead to 100 % liquid full conditions at the opening of the reclosing pressure relief device.

5 Two-phase Flow Dynamics

Consider a vessel containing a two-phase mixture with an adequately sized relief device. The vapor space is maintained at a pressure that is above the bubble point of the liquid through the use of a nitrogen pad, i.e. the system is subcooled. Let us assume that a puncture / line break develops in the vapor space or the relief device is actuated due to external fire or internal chemical reaction.

We expect that mostly nitrogen will be vented first and the pressure in the vapor space to start decreasing. As the pressure reaches the bubble point, the liquid starts to flash and vapor bubbles are formed. As a result the liquid level swells (expands), and depending on the initial fill level and the liquid characteristics, the swell level can reach the relief device or puncture/break point and a two-phase mixture is discharged. If the liquid is cooled or tempered as it flashes to vapor, i.e. internal energy is converted to vaporization energy, the system is referred to as tempered.

As previously discussed, another mechanism by which two-phase flow can occur for top vessel venting or discharge is when the superficial vapor velocity at the relief device or break entrance is higher than the liquid entrainment velocity, and thus the liquid droplets are carried into the relief device or break entrance. This is mostly important for high liquid fill levels or vessels with

Table 1: Maximum permissible liquid fill level for a 25,000 gal rail car transport at normal fill conditions of 68 °F

	n-Butyl Acrylate	Methyl Methacrylate	Vinyl Acetate	Acetone	Ethanol
Normal Boiling Point, °F	298.13	212.54	162.50	133.32	172.92
Saturation Temperature, °F	566.94	468.02	381.94	346.60	349.09
Critical Temperature, °F	616.73	555.53	483.53	455.09	469.58
Set Pressure, psig	250.00	250.00	250.00	250.00	250.00
Critical Pressure, psig	366.75	519.04	601.71	667.20	911.15
Saturated Liquid Density, kg/m^3	505.97	612.32	655.19	567.92	604.06
Liquid Density @68 F kg/m3	898.92	942.52	932.28	791.19	791.74
Maximum Fill Level @68 °F %	56.29	64.97	70.28	71.78	76.29
Total Mass, lbs	105,549	127,735	136,679	118,473	126,011
	1,3-Butadiene	Vinyl Chloride	Water	Propane	Ammonia
Normal Boiling Point, °F	24.06	7.93	212.00	-43.67	-28.17
Saturation Temperature, °F	216.59	192.11	406.21	127.41	114.74
Critical Temperature, °F	306.00	317.93	705.16	206.01	270.50
Set Pressure, psig	250.00	250.00	250.00	250.00	250.00
Critical Pressure, psig	613.30	807.67	3184.11	601.60	1620.97
Saturated Liquid Density, kg/m^3	493.74	774.17	857.55	443.61	568.57
Liquid Density @68 F kg/m3	620.85	911.17	996.42	500.78	608.86
Maximum Fill Level @68 °F %	79.53	84.97	86.06	88.58	93.38
Total Mass, lbs	102,998	161,500	178,892	92,541	118,609

oversized relief devices.

Under some vessel conditions the vapor could disengage completely from the liquid inside the vessel so that the swelled liquid level remains below the discharge point and all vapor flow occurs. This is referred to as partial vapor disengagement and can happen as soon as the relief device or break occurs or after a certain period of two-phase flow. Foamy liquids exhibit little vapor disengagement and as a result a large portion of the vessel contents is vented as a two-phase mixture. It is difficult to determine a priori whether or not a fluid is foamy. This is best done by testing using calorimetry or other suitable means. In general, foaming in chemical mixtures is enhanced by a large difference in surface tension of the mixture components [1].

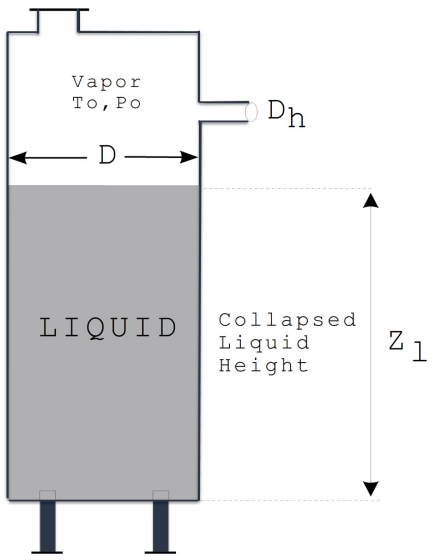

The level of liquid swell in the vessel depends on fluid char-

acteristics, flow regime and dynamics of bubble rise and liquid disengagement. The bubble rise velocity depends on buoyancy and surface tension and is retarded by the viscosity and foaminess of the liquid. Typical flow regimes include:

1. bubbly flow,
2. churn-turbulent, and
3. droplet flow.

When non-condensible gases are generated due to chemical reaction, the system is referred to as gassy. For foamy liquids, i.e. where the liquid phase remains continuous to essentially 100 % void fraction, the discharge should be assumed to be homogeneous two-phase at all times.

6 Simple Methods for Onset/Disengagement

A simple method for onset/disengagement is presented by Fauske [2] for non-foamy materials. Vapor flow occurs around a void fraction of 50 %:

$$z_l \quad < \quad \frac{z_h}{2} \tag{2}$$

Two phase flow occurs when:

$$0.6 \left(\frac{D_h}{D} \right)^2 \sqrt{R_g T_0 / M_w} \quad > \quad u_\infty \left[\frac{z_h - z_l}{z_h} \right] \left[\frac{z_l}{z_h} \right] \tag{3}$$

where

$$u_\infty \quad = \quad 1.20 \frac{\left[\sigma g \left(\rho_l - \rho_v \right) \right]^{0.25}}{\sqrt{\rho_l}} \tag{4}$$

The left hand side of Equation 3 is the vessel superficial vapor velocity based on choked flow through the hole and the right hand side is the characteristics two-phase drift velocity for bubbly flow.

Bubbly flow regimes are more likely in typical process vessels because they are favored by the presence of small quantities of impurities, while for example churn-turbulent flow is typical for clean water-like flow conditions.

7 The DIERS Coupling Equation

A more detailed method for predicting the onset and disengagement of two-phase flow for non-foamy liquids from a vertical vessel during depressurization or emergency relief was developed and validated by DIERS [3]. Vapor holdup is predicted using a first order lumped parameter drift-flux formulation.

7.1 Two-phase Flow Onset and Disengagement

The vapor-liquid flow regimes that are addressed with this method include bubbly and churn-turbulent. The DIERS method proceeds as follows:

1. Determine the vapor capacity of the relief device or the orifice, $\dot{M}$.

2. Calculate the superficial vapor velocity:

$$u_{sv} = j_{g\infty} = \frac{\dot{M}}{\rho_v A} \tag{5}$$

   where A is the vessel cross sectional area in m^2. Grolmes and Fisher [4] showed that all onset/disengagement models based on constant cross-sectional area for vertical cylindrical geometries can be used with little error for horizontal cylinders and spheres. For a sphere, assume an equivalent vertical cylinder with a cross sectional area equal to 2/3 the area of the sphere (or diameter = 0.8165 times the diameter of the sphere). For a horizontal cylindrical configuration, assume an equivalent vertical cylinder with a diameter equal to the square root of the horizontal cylinder diameter by length. One can also simply divide the total volume by the vertical dimension of the vessel to obtain an equivalent vertical cylindrical vessel cross sectional area.

3. Calculate the bubble rise velocity:

$$u_{\infty} = c\frac{[g\sigma(\rho_l - \rho_v)]^{1/4}}{\sqrt{\rho_l}} \tag{6}$$

   where c is a constant which is flow regime dependent. Its value is 1.53 for churn flow and 1.18 for bubbly flow.

4. Calculate the dimensionless superficial vapor velocity due to flow:

$$\psi_F = \frac{j_{g\infty}}{u_{\infty}} = \frac{u_{sv}}{u_{\infty}} \tag{7}$$

5. Calculate the dimensionless superficial velocity at which two-phase flow commences. For bubbly flow it is:

$$\psi = \frac{\alpha(1-\alpha)^2}{(1-\alpha^3)(1-C_0\alpha)} \tag{8}$$

where α is the vessel average void fraction and C_0 is a correlating parameter determined from experimental data. Its value ranges from 1.01 (conservative) to 1.2 (best estimate).

For churn flow, ψ is given by:

$$\psi = \frac{2\alpha}{1-C_0\alpha} \tag{9}$$

The value of C_0 ranges from 1 (conservative) to 1.5 (best estimate).

6. If $\psi_F \geq \psi$, two-phase flow is predicted.
If $\psi_F < \psi$ vapor flow is predicted.
If $\psi_F < \psi$ and two-phase flow is in progress, disengagement is predicted.

The α vs. ψ curve is shown in Figure 15. To determine if a particular vapor venting rate will result in two-phase flow, one can simply locate the associated ψ and void fraction point on the chart. If the point is above the selected flow regime curve, then all vapor flow is predicted. If the point is below the curve, then two-phase flow will occur. Note that the purple curve (Co=1.20, Actual - Bubbly) represents the results of a dynamic vessel simulation consisting of many α vs. ψ points throughout the simulation.

7.2 Vapor Quality Entering Vent

If two-phase flow conditions are predicted, the weight fraction of vapor entering the relief device or break is the one which satisfies the following relation:

$$\frac{\mathcal{Y}G_m A_h}{\epsilon\zeta u_\infty \rho_v A} = \frac{1}{1-C_0\epsilon\frac{\rho_v}{\rho_l}\frac{1-\mathcal{Y}}{\mathcal{Y}}} \tag{10}$$

where ϵ and ζ are flow dependent parameters given as function of the vessel average void fraction. This equation is often referred to as the DIERS coupling equation. For bubbly flow:

$$\epsilon = \frac{\alpha}{1-C_0\alpha} \text{ and } \zeta = \frac{(1-\alpha)^2}{1-\alpha^3} \tag{11}$$

For churn flow:

$$\epsilon = \frac{2\alpha}{1-C_0\alpha} \text{ and } \zeta = 1 \tag{12}$$

Calculations involving partial vapor-liquid disengagement can be computationally intensive as they require calculation of G at each estimate of $\mathcal{Y}$. Note that at very large superficial vapor velocities (large vents), the disengagement will occur at a vessel liquid level equal to $\left(\frac{C_0-1}{C_0}\right)$.

8 Solving the Coupling Equation

The solution of the DIERS coupling equation requires trial and error. The form represented by Equation 10 has to be rearranged in order to produce a solution without numerical discontinuities as shown by Melhem [5, 6]. The preferred form for a numerical solution is:

$$f(\mathcal{Y}) = G_m \left(\frac{A_h}{A}\right)\left(\mathcal{Y} - C_0\epsilon\frac{\rho_v}{\rho_l}(1-\mathcal{Y})\right) - \epsilon\zeta u_\infty \rho_v = 0 \tag{13}$$

The solution begins by guessing the vapor quality entering the vent, $\mathcal{Y}$, and then by estimating the mass flow through the vent, G_m, using an appropriate two-phase flow model (often homogeneous equilibrium). The calculated value of G_m is inserted in Equation 13 and $f(\mathcal{Y})$ is then evaluated. With this form of the DIERS coupling equation the actual solution of $\mathcal{Y}$ will always be bounded between 0 and 1.

9 Application of the Coupling Equation to Quench Tanks

The level swell in a quench tank which involves gas/vapor bottom sparging instead of volumetric gas generation can be determined from the following equation for ψ:

$$\psi = \frac{\alpha}{1 - C_0\alpha} \tag{14}$$

This equation [7] uses the non-integral form of the churn turbulent drift flux relationship (see Zuber [8] and Wallis [9]). It will predict more level swell than Equation 9 since the maximum gas rate occurs throughout the entire two-phase column.

The DIERS coupling equation only predicts two-phase flow due to level swell. In order to account for two-phase flow due to liquid entrainment caused by gas bubbling through the liquid column, the following relation is typically used (also see [10]):

$$\frac{\dot{m}_{liq}}{\dot{M}_{gas}} = 0.18\frac{u_{sv}^3\rho_v^{1.5}}{\left[g(\rho_l - \rho_v)\sigma\right]^{\frac{3}{4}}} \tag{15}$$

where $\dot{m}_{liq}$ is the liquid entrainment rate in kg/s. Note that two-phase flow caused by level swell will not occur simultaneously with two-phase flow caused by liquid entrainment. If the swell does not reach the vessel top, only liquid entrainment will occur. If the swell reaches the vessel top, liquid entrainment will not occur.

Figure 2: Non-boiling height considerations

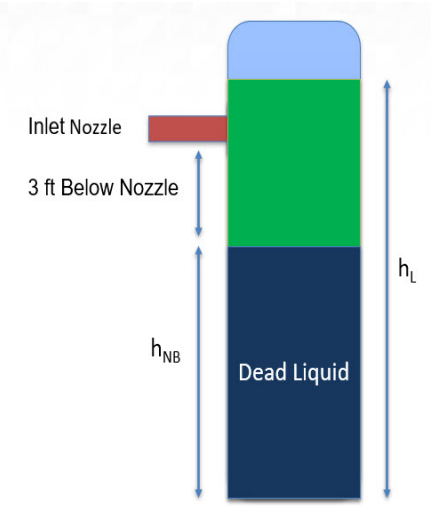

10 Non-boiling Height Considerations

The DIERS coupling equation key parameters include the average void fraction in the swelled liquid, the superficial vapor velocity at the liquid surface, and the bubble rise velocity [11]. There are practical scenarios where boiling and/or vapor generation does not occur throughout the entire liquid volume but only occurs at the top portion of the liquid. As a result, liquid swell does not occur below the top liquid portion because the bottom liquid portion does not contain bubbles. The churn-turbulent model can be extended to handle top-biased vapor generation by using the average void fraction of the top portion of the liquid, $\hat{\alpha}$. This is referred to as the nonboiling height vessel model. The same value of ψ is used in the DIERS coupling equation, but with $\hat{\alpha}$:

$$\psi = \frac{2\hat{\alpha}}{1 - C_0\hat{\alpha}} \tag{16}$$

$$\hat{\alpha} = \frac{\alpha}{1 + \delta\,(\alpha - 1)} \tag{17}$$

where α is the vessel overall average void fraction, and δ is the ratio of nonboiling liquid region height to the unaerated rest height of the total liquid. Although the physical basis for nonboiling height is not directly applicable to gas sparged systems, a reasonable value of δ can be specified to reflect the location where the gas is being sparged into the liquid relative to overall liquid height.

Where there is a physical basis for determining the nonboiling liquid height due to strong recirculation effects in the boiling region caused by rising vapor bubbles, δ can be approximated from:

$$\delta = \frac{1}{1 + 0.76\left(\frac{1}{D^{0.2}}\right)\left(\frac{1}{\rho_l}\right)\left(\frac{dP_s}{dt}\right)} \tag{18}$$

where D is the vessel diameter in meters, ρ_l is the liquid density in $\mathrm{kg/m^3}$, and $\frac{dP_s}{dt}$ is the rate of saturation pressure change with time in $\mathrm{Pa/s}$ during venting. Effectively, the non-boiling height model causes the churn turbulent model to be executed with a higher value of α which leads to quicker vapor/liquid disengagement.

The non-boiling height model can be extended to applications where vapor is introduced below the liquid level through a nozzle or a pipe. In this application the liquid towards the bottom of the vessel is considered to be "dead" liquid without any bubbles. The values of δ can be set at:

$$\delta = \frac{h_{NB}}{h_L} \tag{19}$$

The "dead" liquid layer has to be clear of bubbles from any internal or external sources. Instead of using 3 ft below the nozzle, one can approximate the gas penetration depth as the point at which the horizontal velocity of the incoming gas and entrained liquid equals the bubble rise velocity from Equation 6 for churn turbulent flow.

11 Wall Heating Considerations for Low Pressure Vessels

Venting requirements for large low pressure storage vessels containing non foamy and non reactive chemicals are typically based on all vapor flow. The potential occurrence of liquid swell due to external heating can lead to two phase flow and substantially increased venting requirements.

Figure 3: Wall heating considerations

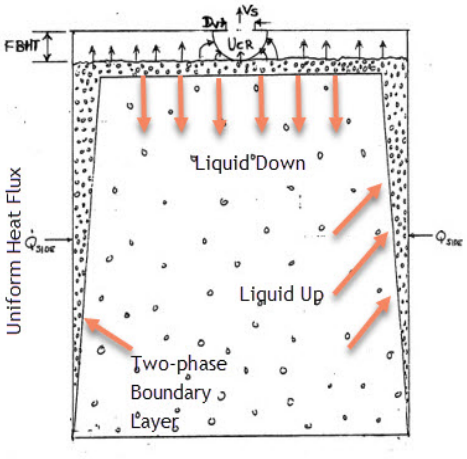

While the time required for sustained venting can be based on bulk heating, for large vessels under wall heating, sustained venting will only occur when the bulk liquid has reached saturation conditions [4]. Under wall heating, the highest temperature fluid will tend to accumulate in the upper regions of the vessel. This will cause the vapor space pressure to increase sooner and cause intermittent venting until bulk saturation conditions are reached [12]. Without bulk mixing, liquid in the lower portions of the vessel can become highly subcooled. Strong boiling induced convective flows can promote bulk mixing which minimizes thermal gradients.

Boiling from heated surfaces can cause stronger convective flows than those encountered in single phase free convection. Wall heating causes the formation of vapor bubbles along the wall surface. The vapor bubbles break away from the wall surface and rise along the wall. The vapor causes liquid to also move upwards because of vapor/liquid drag. This leads to the formation of a two-phase free convective boundary layer.

Another variation to the DIERS coupling equation was proposed by Fisher and Forrest [13] for large vessels under fire exposure where bubble generation only occurs at the walls.

This model applies where the bottom of the large vessel is not exposed to fire such as large flat bottom tanks designed per API 620/650 where the fire can only heat the side walls.

This model does not apply to mixtures that are chemically reactive, mixtures that are viscous, or where gas is being sparged or bubbled into the liquid. A new definition of void fraction required to avoid two-phase flow due to wall heating is provided:

$$\delta(x) = \beta \times x \tag{20}$$

$$\hat{\alpha} = 2 \times \alpha_{BL} \times \frac{\delta(H_l)}{D} = 2 \times \alpha_{BL} \times \frac{\beta \times H_l}{D} \tag{21}$$

$$\beta = 0.089 + 0.0322 \times J_o \tag{22}$$

$$\alpha_{BL} = 0.5354 \times J_o^{2/3} \tag{23}$$

$$J_o = \frac{q_w}{\rho_v u_\infty \lambda} \tag{24}$$

where J_o is a dimensionless wall heat flux (see [7] Appendix C), $\hat{\alpha}$ is the average void fraction over the vessel liquid pool, α_{BL} is the average void fraction in the boundary layer, β is the boundary

[4] Typically, the coincident temperature of the relief device set pressure.

layer thickness growth rate, $\delta(x)$ is the boundary layer thickness as a function of vertical distance x (or liquid height), H_l is the liquid height in the vessel, D is the vessel diameter, q_w is the fire flux [5] in $\mathrm{W/m^2}$, ρ_v is the vapor density in $\mathrm{kg/m^3}$, u_∞ is the chrun turbulent flow regime bubble rise velocity defined in Equation 6 in $\mathrm{m/s}$, and λ is the latent heat of vaporization in $\mathrm{J/kg}$.

We note that the temperature rise rate for the boundary layer, $\frac{dT_{bl}}{dt}$, is directly proportional to the ratio of the wetted surface area of the vessel to the volume of the boundary layer:

$$\frac{dT_{bl}}{dt} = \left(\frac{q_w}{\rho c_p}\right)\frac{A_w}{V_{bl}} \tag{25}$$

for a vertical cylindrical vessel,

$$\frac{dT_{bl}}{dt} = \left(\frac{q_w}{\rho c_p}\right)\frac{2\pi D H_l}{\pi D H_l \delta(H_l)} = \left(\frac{q_w}{\rho c_p}\right)\frac{2}{\delta(H_l)} \tag{26}$$

This means that the initial rate of pressure rise in the vessel which depends on the rate of temperature rise for the boundary layer will be higher for vessels with smaller boundary layer, or smaller vessels.

The temperature rise rate for the bulk liquid, $\frac{dT_{bulk}}{dt}$, is directly proportional to the ratio of the wetted surface area of the vessel to the vessel liquid volume, V_l:

$$\frac{dT_{bulk}}{dt} = \left(\frac{q_w}{\rho c_p}\right)\frac{A_w}{V_l} \tag{27}$$

for a vertical cylindrical vessel,

$$\frac{dT_{bulk}}{dt} = \left(\frac{q_w}{\rho c_p}\right)\frac{4\pi D H_l}{\pi D^2 H_l} = \left(\frac{q_w}{\rho c_p}\right)\frac{4}{D} \tag{28}$$

The above equation indicates that larger vessels will heat slower assuming the same fill level. The boundary layer change in temperature relative to the change in temperature of the bulk liquid is proportional to the total liquid volume divided by the boundary layer volume:

$$\frac{dT_{bl}}{dT_{bulk}} = \frac{V_l}{V_{bl}} \text{ or } \frac{dT_{bl}}{dT_{bulk}} = \frac{D}{2\delta\left(H_l\right)} = \frac{D}{2\beta H_l} \text{ for a vertical cylindrical vessel.} \tag{29}$$

At a value of $J_o = 0.3$, β is approximately equal to 0.1 which leads to:

$$\frac{dT_{bl}}{dT_{bulk}} = \frac{D}{0.2H_l} \text{ for a vertical cylindrical vessel.} \tag{30}$$

At high values of J_o we would expect the rate of temperature rise due to boundary layer heating to equal the rate of temperature rise due to bulk heat at liquid level to diameter ratio of 5 for a vertical cylindrical vessel.

[5] Depending on what simulation method is used, q_w may require the computation of vessel wetted area at relief temperature, which in turns requires the computation of the void fraction needed to avoid two-phase flow.

$\hat{\alpha}$ will be smaller than an overall average void fraction, α, based on conversion of the external heat flux to a specific volume source:

$$\psi = F \times J_o \times \frac{H_l}{D} \tag{31}$$

$$\alpha = \frac{\psi}{2+\psi} \tag{32}$$

where ψ is a dimensionless uniform source and F is a shape factor. $F = 6$ for a sphere, $F = 4$ for a vertical cylindrical shape, and $F = \frac{\frac{L}{D}+1}{3\frac{L}{D}+2}$ for a horizontal cylinder. L/D is the length to diameter ratio of the horizontal cylinder.

Fisher and Forrest [13] further modified the vapor/liquid disengagement criteria by defining a void fraction required to avoid two-phase flow due to liquid entrainment:

$$\alpha_{ent} = \frac{F_{BHT}}{H_{tank}} \tag{33}$$

$$F_{BHT} = R_v\sqrt{\frac{u}{2u_e}} \tag{34}$$

where R_v is the relief device flow radius, u_e is the critical liquid entrainment velocity defined in Equation 55, F_{BHT} is the required free board height in the vessel to avoid liquid entrainment, H_{tank} is the tank height, and u is the pseudo vent discharge gas velocity $\frac{\dot{m}_g}{\rho_g A_v}$.

Two-phase flow is predicted if:

$$(1-\alpha_o) + (1-\alpha_{ent})\,\hat{\alpha} + \alpha_{ent} \geq 1 \tag{35}$$

where α_o is the overall vessel average void fraction, $\alpha_o = \frac{V_T - V_l}{V_T}$. The free board height relation (see equation 34) is derived by assuming that the flow through the imaginary surface area of half sphere of radius F_{BHT} at the entrance of the vent is equal to the vent flow at entrainment:

$$2\pi F_{BHT}^2 u_e = \pi R_v^2 u \tag{36}$$

$$F_{BHT} = \frac{\pi R_v^2 u}{2\pi u_e} = R_v\sqrt{\frac{u}{2u_e}} \tag{37}$$

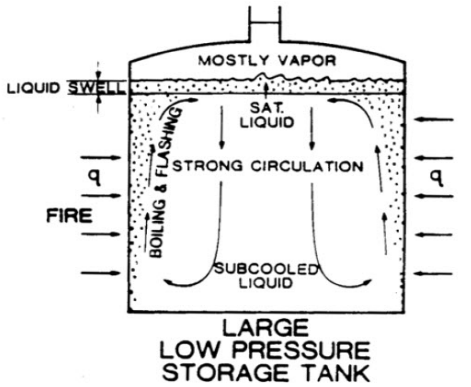

Source: [14]

The original analytical work on wall heating considerations for large atmospheric low pressure storage vessels was carried out by DIERS in the early 1980s [7, 14, 15].

Equations 21-24 were initially presented by Grolmes [15, 7] with additional considerations for vapor bubble carry-under based on hydrodynamic considerations, which increased the potential

for two phase flow due to wall heating. Later on, Fauske [14] demonstrated that subcooling caused by a small static liquid head, H_{sc}, will result in the collapse of vapor bubbles dragged or carried under by the recirculating flow:

$$H_{sc} \simeq \frac{\lambda^2 \rho_v^2 \alpha}{c_p T \rho_l^2 (1-\alpha)(1-\bar{\alpha}) g} \tag{38}$$

where α is the void fraction at the top of the liquid pool in the vessel, $\bar{\alpha}$ is the average void fraction, T is the saturation temperature, g is the gravitational constant, c_p is the liquid specific heat, and H_{sc} is the liquid height that is required to cause the collapse of the vapor bubbles.

Fauske recommended that the all vapor venting flow area should be large enough to prevent liquid entrainment by ensuring that the vapor velocity in the vent line is kept below the entrainment velocity, u_e (see Equation 55):

$$A_v = \frac{\dot{Q}_{fire}}{\lambda \rho_v u_e} \tag{39}$$

where A_v is the required vent area and $\dot{Q}_{fire}$ is total heating rate provided by the fire. Fauske [14] suggests that increasing A_v in Equation 39 by a factor of 2 would keep the overpressure to approximately 0.1 psi even for a foamy system. In case where higher overpressure can be tolerated, Fauske [14] recommends replacing u_e in Equation 39 by:

$$u \simeq \frac{\Delta P}{\rho_v} \tag{40}$$

where ΔP is the overpressure.

Wall heating dynamics are also included in Process Safety Office® SuperChems Expert™. We note that the DIERS coupling equation does not need to be solved in this particular case to determine the vapor quality entering the vent line. Instead, the vapor quality entering the vent line is set to a value such that the void fraction entering the vent line, $\alpha_{\text{vent inlet}}$ is equal to the void fraction provided in the following equation:

$$\alpha_{\text{vent inlet}} = (1-\alpha_{ent})\,\alpha_{wall} + \alpha_{ent} \tag{41}$$

$$a_C = \frac{V_l}{V_v}\left(\frac{\alpha_{\text{vent inlet}}}{1-\alpha_{\text{vent inlet}}}\right) \tag{42}$$

$$y = \frac{a_C N_v}{a_C N_v + N l} \tag{43}$$

where y is the vapor to liquid molar ratio entering the vent line, N_l is the total number of liquid moles in the vessel, and N_v is to the total number of vapor moles in the vessel.

12 Simpson's Method for Vessels Rated at ≥ 15 psig

Simpson [16] developed simple criteria for when all vapor venting will be adequate even when the liquid level is high enough to initially cause two phase flow. His criteria are applicable to non-viscous and churn-turbulent like systems where agitation and chemical reactions are not occurring. Simpson's criteria is applicable to vessels with pressure ratings higher than 15 psig.

Simpson [16] argues that all vapor venting will be adequate and appropriate when a sufficiently large vapor space can be cleared via two phase flow before the pressure increased from 1.1 to 1.21 times the set pressure of the pressure relief device. Vapor venting only occurs when the dimensionless time, t_s, is greater than 1:

$$t_s = \frac{t_d + t_o}{t_v} > 1 \tag{44}$$

where t_d is the mixing time, t_o is the overpressure time required to increase the pressure from 1.1 to 1.21 the set pressure of the pressure relief device, and t_v is the two phase venting time required to clear the vapor space. t_d and t_o are considered independently because they both involve heat-up periods [16]. Thermal stratification is reducing during t_d and pressure is building during t_o.

t_d refers to the time it takes for the fluid in the vessel to achieve a relatively uniform temperature distribution solely due to the movement generated by natural convection, where warmer fluid rises and cooler fluid sinks, creating circulation and mixing [6] within the vessel. Direct expressions for t_d are not generally available because of system specific complex fluid patterns and dynamics. We note that many factors affect the mixing time including:

Temperature difference: Larger temperature gradients lead to faster mixing due to stronger buoyant forces.

Fluid properties: Fluids with higher thermal expansion coefficients and lower viscosity will mix faster.

Vessel geometry and size: Vertical vessels generally have faster mixing than horizontal ones due to gravity-driven flow. Larger vessels typically take longer to mix due to longer flow paths.

Computational fluid dynamics can be used to determine credible and relatively precise mixing time values. However, it is not yet practical to perform these types of calculations for multiphase flow dynamics, especially where choked flow occurs during relief and a single volume (lumped parameter) approach remains the largely preferred option [17]. Another method for estimation of approximate mixing times is to use semi-empirical correlations developed from mixing time measurements such as the one proposed by Simpson:

$$t_d = 79.2 D^{0.788} \tag{45}$$

where t_d is the approximate mixing time in seconds and D is the vessel diameter in ft. Equation 45 was developed based on a limited data set measured by Birk [18, 19] for vertical LPG vessels under

[6] Relief device actuation can also cause mixing to occur during relief.

fire exposure. Equation 45 represents the time required for de-stratification of the bulk liquid due to relief device actuation and bulk generation of vapor bubbles as the vessel is depressuring.

13 Destratification Time

Destratification is enhanced by the opening of pressure relief valves with large blowdowns. Stratification has not been observed in vessels where the liquid level is low or for vessels where the top vessel surface is shielded from thermal radiation.

Equation 45 indicates that it takes longer to destratify a larger vessel than a smaller vessel. However, Equation 45 may not be applicable to fluids and mixtures where the Rayleigh number, R_a, is much larger than that of Birk's limited test data set. A larger R_a value indicates more vigorous convection which results in faster fluid mixing since the Rayleigh number is a measure of ratio of buoyancy forces driving convection to viscous forces opposing and resisting mixing. For free convection near a vertical wall, R_a is defined as:

$$R_a = \frac{g\beta}{\nu\alpha}\left(T_s - T_\infty\right)x^3 \tag{46}$$

where x is a characteristic length, g is the acceleration due to gravity, β is the thermal expansion coefficient, ν is the kinematic viscosity, α is the thermal diffusivity, T_s is the surface temperature, and T_∞ is the fluid temperature far from the surface. The properties in 46 are typically evaluated at the film temperature,T_f, which is given by: $T_f = \frac{T_s+T_\infty}{2}$.

Figure 4: Predictive model performance for destratification time, t_d

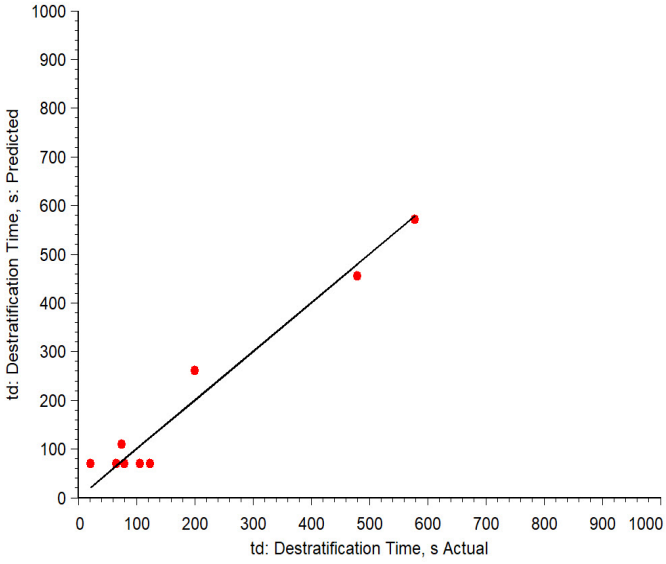

Source: SuperChems Expert

Since we are interested in heat transfer to the fluid in the vessel from fire exposure or a heating jacket, it is more appropriate to represent R_a as a function of a wall heat flux [20]:

$$R_a = \frac{g\beta_l\rho_l^2 c_{p,l}}{k_l^2\mu_l}q_w H_l^4 = \frac{g\beta_l}{\mu_l\alpha_l^2}\frac{q_w}{c_{p,l}}H_l^4 \tag{47}$$

where R_a is a modified Rayleigh number, k_l is the liquid thermal conductivity, μ_l is the liquid viscosity, H_l is liquid height, ρ_l is the liquid mass density, and $c_{p,l}$ is the liquid specific heat at constant pressure.

Equation 45 can be scaled to include the effects of fluid properties on the mixing time t_d:

$$t_d = 79.2D^{0.788} \times \frac{R_{a,Birk}}{R_a} \tag{48}$$

Simpson's Equation 45 should not be used for fluids that have different properties than LPG/propane because the criteria outlined by Equation 44 which depends on the value of t_d may not be adequate enough to justify the use of all vapor venting only for relief requirement.

More recently, Hendrickson [7] analyzed several large scale data sets including the propane data used by Simpson to develop Equation 45 as well as additional LNG data. This data set was further analyzed by the SuperChems Expert data mining and predictive modeling [21] tools and it shows a very strong dependency on vessel diameter and dimensionless wall heat flux with low degree of inter-correlation between the independent variables:

$$t_d = 308.5 D^{0.788} - 5,932 J_o \tag{49}$$

where t_d is in s, D is in m, and J_o is dimensionless.

Hendrickson developed a correlation for the estimation of t_d but excluded data points with high PRV blowdowns. A dimensionless destratification number, N_d, is correlated with Rayleigh and Reynolds numbers:

$$R_e = \frac{D u_\infty \rho_l}{\mu_l} \tag{50}$$

$$R_a = \frac{g \beta \rho_l^2 c_{p,l}}{k_l^2 \mu_l} q_w H_l^4 \tag{51}$$

$$N_d = 4 t_d J_o \frac{\rho_v}{\rho_{l,o}} \frac{u_\infty}{D} = 35.67 \times \frac{R_a^{0.415}}{R_e^{1.634}} \text{ or } t_d = 8.92 \times \frac{R_a^{0.415}}{R_e^{1.634}} \times \rho_{l,o} \frac{\lambda}{q_w} D \tag{52}$$

where $\rho_{l,o}$ is the initial liquid mass density, R_e is the Reynolds number, and N_d is a dimensionless destratification time. It is interesting to note that Equation 52 shows almost a linear dependency on vessel diameter when the liquid level, H_l, approaches the vessel diameter since $0.415 \times 4 \simeq 1.634$. Higher values of q_w yield shorter destratification times while higher values of λ and/or denser liquids yield longer destratification times.

14 Liquid entrainment During Vessel Blowdown

Liquid can also be entrained during vessel blowdown if the liquid level is high enough and the gas/vapor velocity in the plane of the vent is high enough. Liquid is entrained from the liquid surface by the gas motion induced by vessel blowdown through vents in the vapor space above the liquid surface (see Figure 5). A semi-empirical relationship for predicting the onset and magnitude of liquid entrainment can be used to determine the ratio of the entrained liquid flow rate to the gas flow rate discharged from the vent:

$$\frac{\dot{m}_{l,e}}{\dot{m}_g} = E_0 \left(\frac{\rho_l}{\rho_g} \right)^{0.5} \left(\frac{R_v}{H} \right) \left[\frac{1}{2} \frac{u}{u_e} \frac{R_v}{H} - 1 \right] \tag{53}$$

[7] See G. Hendrickson, "Liquid Thermal Stratification and destratification in Fire Exposed Pressure Vessels", Revision 2, DIERS Presentation, Spring Meeting, 2025

where $\dot{m}_{l,e}$ is the entrained liquid mass flow rate, $\dot{m}_g$ is the gas mass flow rate, E_0 is an entrainment coefficient ($\simeq 0.1$), ρ_l is the liquid density, ρ_g is the gas density (at vessel conditions), R_v is the vent radius, H is the freeboard (vertical distance between vent plane and liquid interface), u is the pseudo vent discharge gas velocity $\frac{\dot{m}_g}{\rho_g A_v}$ or the gas velocity in the plane of the vent where the flow is considered to become uniform, and u_e is the minimum entrainment velocity.

The last term on the right hand side of Equation 53 must be positive. As a result, a minimum freeboard required for entrainment can be established:

$$H_b = u\left(\frac{R_v}{2u_e}\right) = \left(\frac{\dot{m}_g}{\rho_g A_v}\right)\left(\frac{R_v}{2u_e}\right) \tag{54}$$

where H_b is the free board height required for the onset of entrainment. The minimum velocity required for entrainment, u_e is given by:

$$u_e = 3.1\left[\frac{\sigma g\left(\rho_l - \rho_g\right)}{\rho_g^2}\right]^{1/4} \tag{55}$$

where σ is the liquid surface tension and g is the gravitational constant. Equation 53 can be used in conjunction with a transient blowdown simulation to calculate the liquid entrainment rate as a function of time. Some literature references have applied Equation 53 to estimate the amount of liquid that is aerosolized in deflagrations occurring in the vapor space of vessels containing liquids (see [22], [23], and [24]). Equation 55 was simplified to isolate the contribution of liquid viscosity:

$$u_e = k_g\left[\frac{\sigma g\left(\rho_l - \rho_g\right)}{\rho_g^2}\right]^{\frac{1}{4}} \quad \text{where} \quad k_g = \frac{1}{N_\mu^{0.2}} \tag{56}$$

$$N_\mu = \frac{\mu_l}{\left[\rho_l \sigma\left(\frac{\sigma}{g(\rho_l - \rho_v)}\right)^{\frac{1}{2}}\right]^{\frac{1}{2}}} \tag{57}$$

k_g is a dimensionless numerical constant $\simeq 3.1$ for the onset of droplet entrainment and N_μ is a dimensionless viscosity number which is a measure of how resilient the liquid surface is under turbulent conditions. Note that $k_g = 3.98$ for $N_\mu = 10^{-3}$, $k_g = 2.51$ for $N_\mu = 10^{-2}$, and $k_g = 1.58$ for $N_\mu = 10^{-1}$ respectively. If $\mu_l = 0.5$ cp, $\sigma = 0.02$ N/m, $\rho_l = 496$ kg/m^3, and $\rho_g = 2.88$ kg/m^3, we calculate $N_\mu = 3.52 \times 10^{-3}$, $k_g = 3.095$, and $u_e = 5.7195$ m/s.

Re-entrainment becomes more likely at high operating pressures and as liquid viscosity increases.

15 Void Fraction Limits for Low Pressure Vessels

If we ignore liquid entrainment, Equations 20, 21, 22, 23, 24 and 35 can be reduced to the following limiting value for the overall vessel void fraction necessary to avoid two-phase flow:

$$\alpha_o > 0.03447\frac{H_l}{D}\left[2.764 J_o^{2/3} + J_o^{5/3}\right] \tag{58}$$

Figure 5: Liquid entrainment caused by vessel blowdown

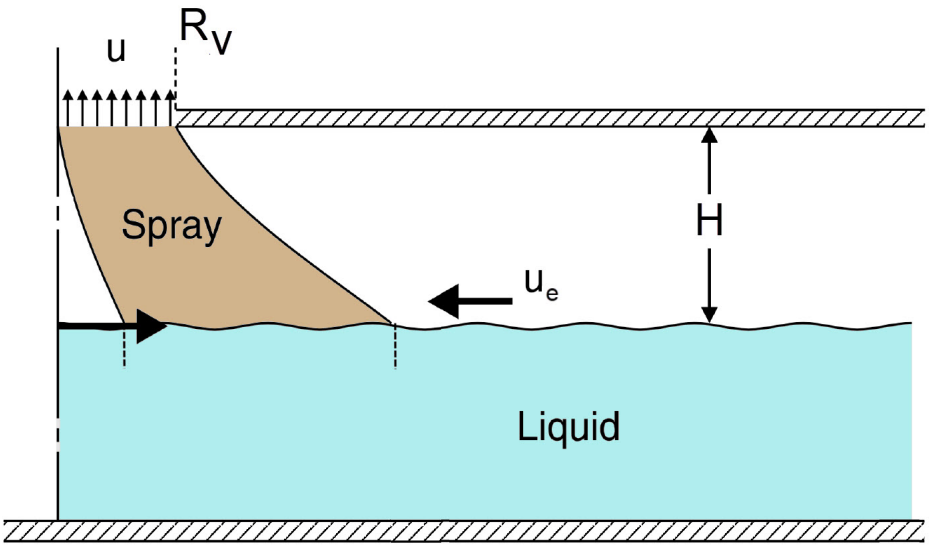

Equation 58 is shown graphically in Figure 6.

As shown in Figure 6, a cryogenic liquid hydrogen storage tank will require a void fraction of approximately 20 % to avoid two phase flow at a dimensionless heat flux value of $J_o = 0.6$ and a height to diameter ratio of 2. A refrigerated ammonia tank with a void fraction of 10 % can tolerate a dimensionless heat flux value of up to $J_o = 0.35$ at a height to diameter ratio of 2. Dimensionless heat flux values for a wide variety of chemicals are shown in Figure 7 as a function of heat flux absorbed by the liquid at normal boiling point conditions.

As shown in Figure 7, a cryogenic liquid hydrogen low pressure storage tank exposed to a heating flux of 60 $\mathrm{kW/m^2}$ will have a dimensionless heat flux value of $J_o = 0.6$ and a refrigerated liquid ammonia tank with a dimensionless heat flux value of $J_o = 0.35$ would have to be absorbing 100 $\mathrm{kW/m^2}$ of heating flux into the liquid.

16 Thermodynamic Consistency of Slip Flow

Nozzle flow where slip exists between the vapor and liquid phases and/or flow from a vessel where the vapor quality entering the vent is different from the vessel average vapor quality are consistent with thermodynamic equilibrium [25]. Simply stated, the vapor and liquid phases can still be in thermodynamic equilibrium at the same temperature and pressure regardless of the relative amount of flowing vapor to flowing liquid. This is true because the individual mole fractions in each phase are still equilibrium mole fractions. The flowing overall composition will be different than the source overall composition and can be easily calculated by combining the vapor and liquid phases

that are in equilibrium:

$$z_i = \frac{x_i\,(1 - x_e) + y_i x_e}{\sum_i \left[x_i\,(1 - x_e) + y_i x_e\right]} \tag{59}$$

where z_i is the overall mass fraction of component i entering the nozzle or vent, y_i is the equilibrium vapor mass fraction, x_i is the equilibrium liquid mass fraction, and x_e is the vapor quality entering the vent. z_i will equal to y_i when $x_e = 1$, x_i when $xe = 0$, and the vessel average composition when x_e is equal to the vessel average vapor quality.

17 Liquid Surface Tension Considerations

The liquid surface tension, σ, is used in the calculation of the bubble rise velocity (see Equation 6). Accurate values can be directly measured and/or obtained from published data for pure components. Mixture data, especially for mixtures with wide boiling point differences or mixtures with non-condensible components such as methane or carbon monoxide or carbon dioxide, should be carefully calculated and must consider the vapor/liquid equilibrium of the mixture at the prevailing system temperature and pressure conditions. An accurate value of mixture surface tension is also important when calculating bubble nucleation rates for non-equilibrium multicomponent two-phase flow, vapor-liquid separator design, rapid phase transitions, and/or rapid vessel blowdown.

One method that can be used and has shown to be reliable is the parachor method. In the simple case of a pure component, σ can be calculated from the following equation:

$$\sigma^{1/n} = \mathcal{P}\,(\rho_l - \rho_v) \tag{60}$$

$$n \simeq 4 \tag{61}$$

where $\mathcal{P}$ is the parachor, σ is the liquid surface tension in $\mathrm{N/m}$, ρ_v is the molar density of vapor in $\mathrm{kmol/m^3}$ in equilibrium with the liquid and ρ_l is the molar density of liquid in $\mathrm{kmol/m^3}$.

Equation 60 can be extended to mixtures:

$$\sigma_m = \left[\sum_i \mathcal{P}_i\,(\rho_{l,m} x_i - \rho_{v,m} y_i)\right]^n \tag{62}$$

$$\mathcal{P}_i = \frac{\sigma_i^{1/n}}{(\rho_{l_i} - \rho_{v_i})} \tag{63}$$

where n ranges between 3.5 and 4.5 but typically set to 4, $\rho_{l,m}$ and $\rho_{v,m}$ are the mixture liquid and vapor molar densities at equilibrium conditions, x_i is the liquid equilibrium mole fraction, and y_i is the vapor equilibrium mole fraction. The mixture vapor/liquid equilibrium conditions are calculated at the bubble pressure or temperature conditions using an equation of state or at constant volume for dynamic vessel relief simulations. Note the parachor value increases sharply when approaching the critical temperature conditions.

Table 2: DIERS Large Scale Test Data Summary

	T2C	T12A
Material	Water	Water + 1000 ppm Detergent
Void Fraction	0.05	0.05
Pressure. kPa	927	510
Flow Type	Nozzle	Nozzle
Vent Location	Top	Top
Discharge Coefficient	1	1
Vent Diameter. mm	32.2	50.8

The parachor [26] may be estimated from the critical properties of a chemical using the following equation:

$$\mathcal{P} \;=\; 0.324\; T_c^{1/4} v_c^{7/8} \tag{64}$$

where T_c is the critical temperature in Kelvin and v_c is the specific molar volume in $\mathrm{m}^3/\mathrm{kmol}$. In general the pure component surface tension depends on reduced temperature:

$$\sigma = \sigma_0 \left(1 - \frac{T}{T_c}\right)^n \tag{65}$$

where n is approximately 1.2, σ_0 is a an empirical constant (in $\mathrm{N/m}$) that can be regressed from measured data or from a reference value of the surface tension, and T is temperature in Kelvin. Note that for polymers, surface tension increases with polymer molecular weight:

$$\sigma = \sigma_\infty - \frac{k_e}{M^{2/3}} \tag{66}$$

where σ_∞ is the polymer surface tension at infinite molecular weight, k_e is a polymer specific constant, and M the polymer molecular weight.

18 Testing the Performance of the Coupling Equation

We consider two DIERS large scale tests [11] using water and water with 1000 ppm of detergent to illustrate the solution and performance of the coupling for churn-turbulent flow (Test T2C) and for bubbly flow (Test T12A). All the solutions for this example were produced using SuperChems Expert.

The vessel used in both tests has a volume of 2190 liters (588 gallons, L=3.048 m, ID=0.9144 m). Details of the tests are shown in Table 2.

Two solutions for Test T2C were produced using SuperChems Expert for Churn Turbulent flow using the recommended DIERS best estimate value of $C_o = 1.5$ and the DIERS recommended

conservative estimate of $C_o = 1.0$. The pressure predictions are shows in Figure 8. A similar pressure profile was predicted in reference [11] for $C_o = 1.5$. The average vessel void fraction estimates are shown in Figure 9. Similar predictions were also reported in reference [11]. A slightly better pressure prediction was reported in reference [11] by using churn turbulent flow with a non-boiling height correction for average void fraction.

The actual numerical solution implementation technique provided in SuperChems Expert is illustrated in Figures 10 and 11 for a single time step. Figure 10 illustrates the behavior of $f(\mathcal{Y})$ as a function of the quantity of vapor entering the vent. We note that $f(\mathcal{Y})$ is well behaved and a solution is easy to obtain.

Figure 11 illustrates the behavior of the DIERS coupling Equation 2 if one attempts to obtain a direct solution of G_m using the coupling equation once $\mathcal{Y}$ is specified. This method of solution has a numerical discontinuity (not shown in Figure 11) and is not reliable.

The results for Test T12A are shown in Figures 12, 13, and 14. All the solutions are performed without a non-boiling height correction. As with Test T2C, similar results are reported in the DIERS Project Manual [11].

Figure 15 superimposes the α vs. ψ calculated by SuperChems Expert for T12A with a $C_o = 1.2$ over the best case and conservative churn turbulent and bubbly α vs. ψ curves. As mentioned earlier, to determine if a particular vapor venting rate will result in two-phase flow, one can simply locate the associated ψ and void fraction point on the chart. If the point is above the selected flow regime curve, then all vapor flow is predicted. If the point is below the curve, then two-phase flow will occur. The purple curve (Co=1.20, Actual - Bubbly) represents the results of T12A dynamic vessel simulation consisting of many α vs. ψ points throughout the simulation.

19 Conclusions

The DIERS coupling equation is an essential modeling tool for the onset/disengagement of two-phase flow. SuperChems Expert includes a detailed implementation of the coupling equation which can used with venting dynamics for simple and complex arrangements of vessels and/or piping. Although the coupling equation can be used to represent if two-phase will onset or disengage at a single specific set of conditions, it is most valuable when used in dynamic simulations of venting and depressuring systems with/without reactions. When used in that context, substantial improvements in process safety and cost effective risk reduction can be realized.

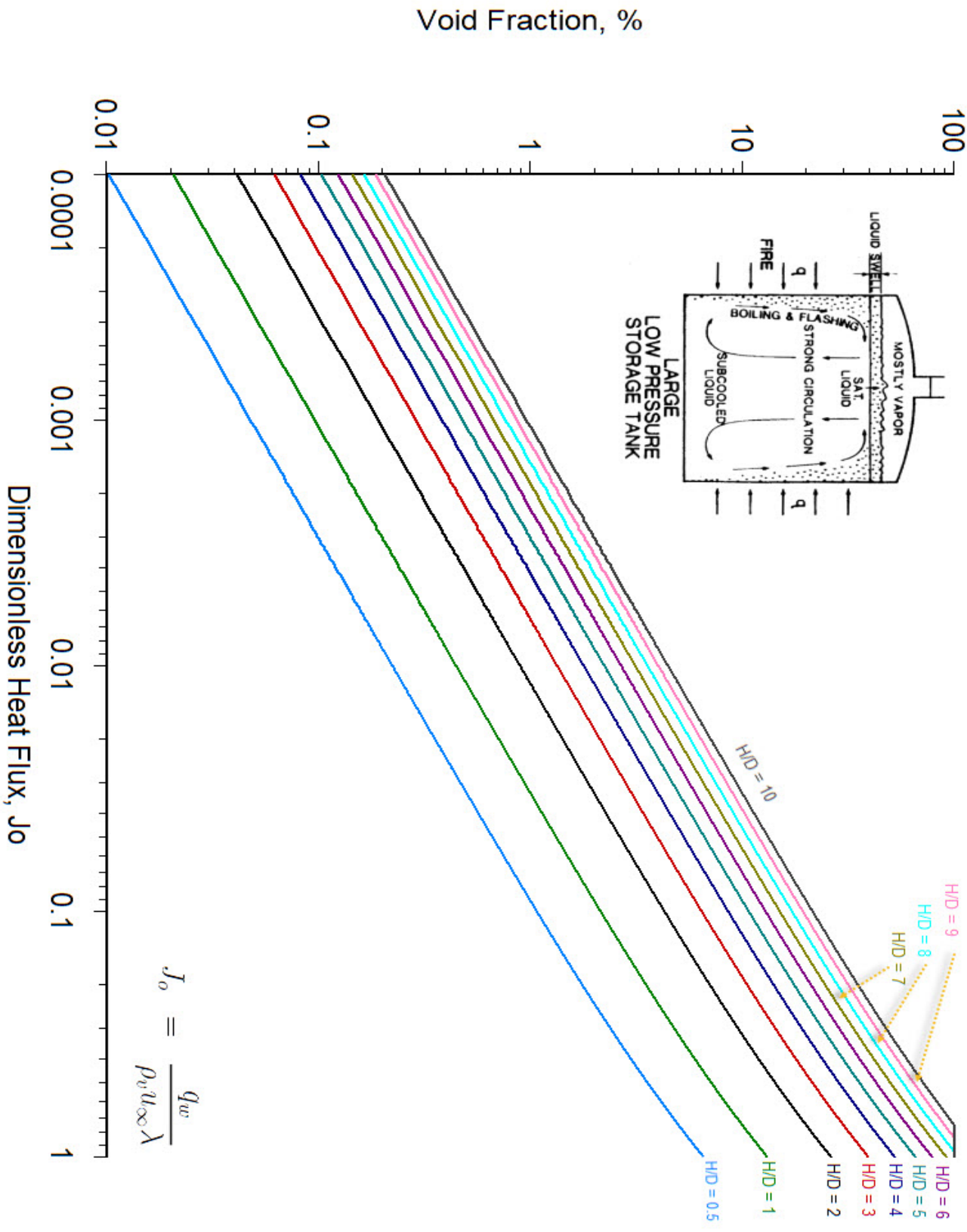

Figure 6: Required overall void fraction to avoid two-phase flow from low pressure vessel vessels subjected to wall heating

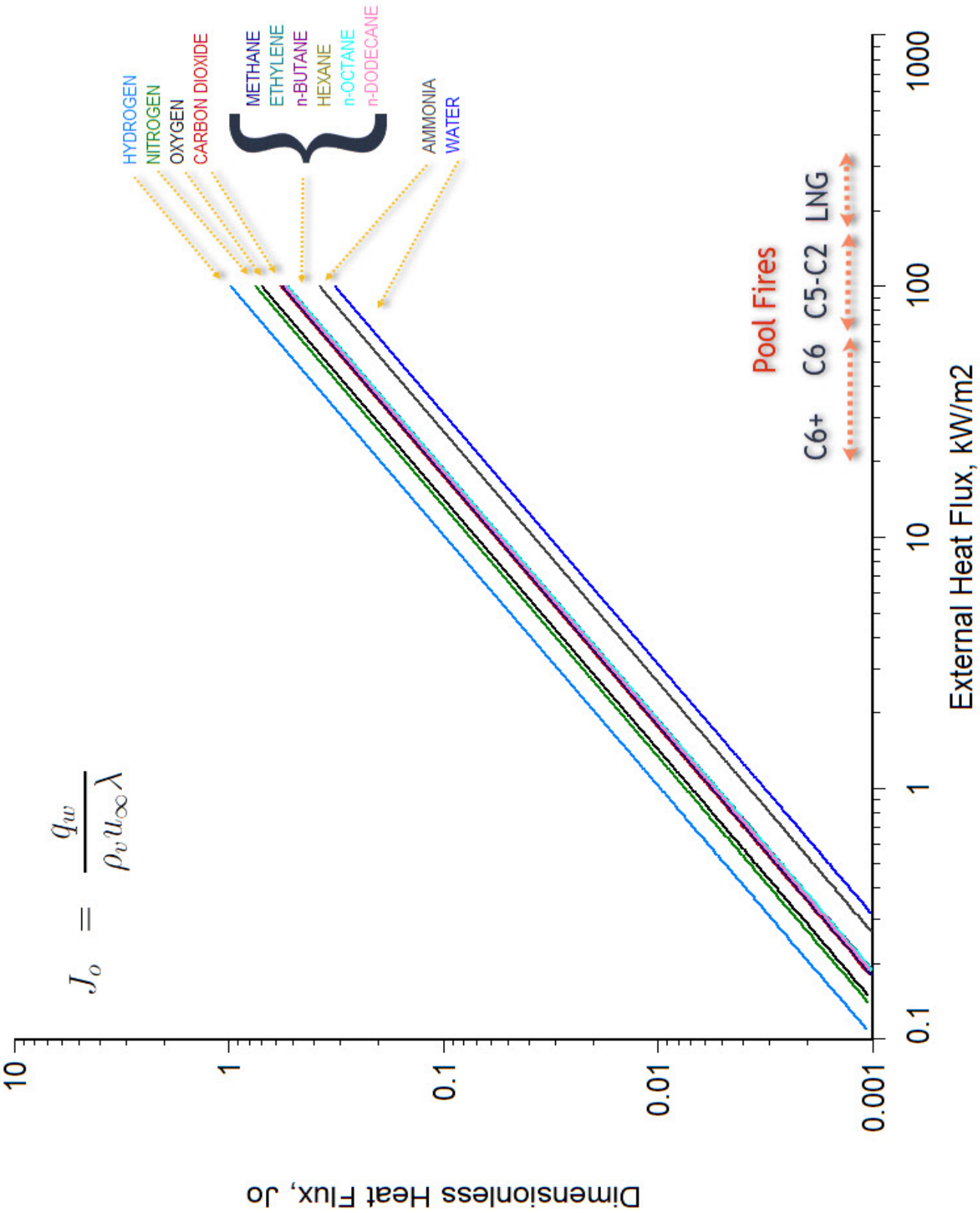

Figure 7: Dimensionless heat flux J_o as a function of heat flux for a wide variety of chemicals at their normal boiling point conditions

Figure 8: SuperChems Expert Churn turbulent estimates of pressure for test T2C

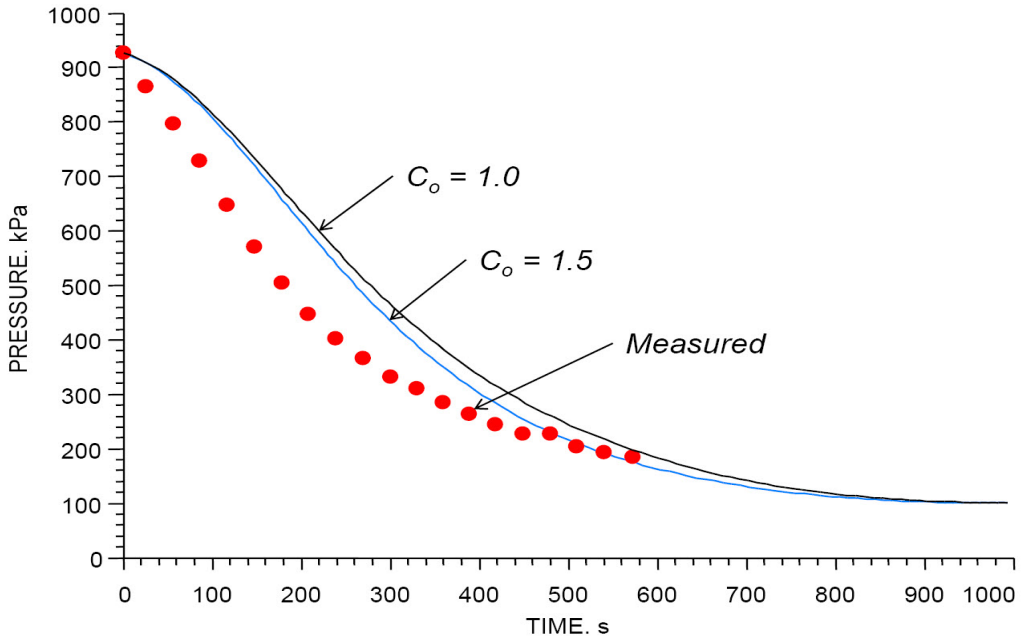

Figure 9: SuperChems Expert Churn turbulent estimates of vessel void fraction for test T2C

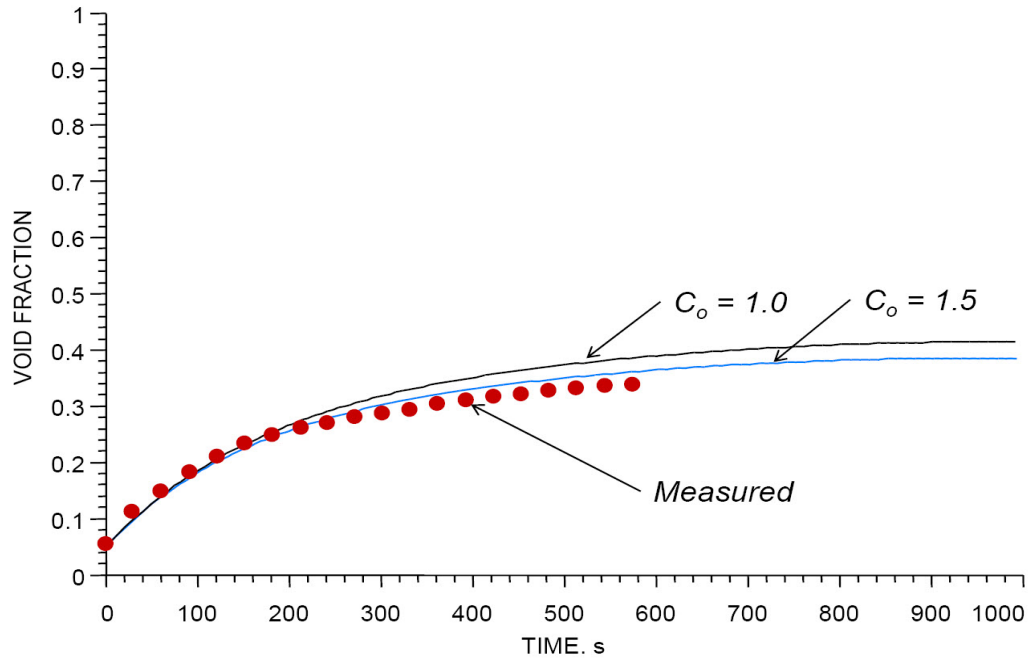

Figure 10: SuperChems Expert Churn turbulent numerical solution of Equation 2 using $f(\mathcal{Y})$

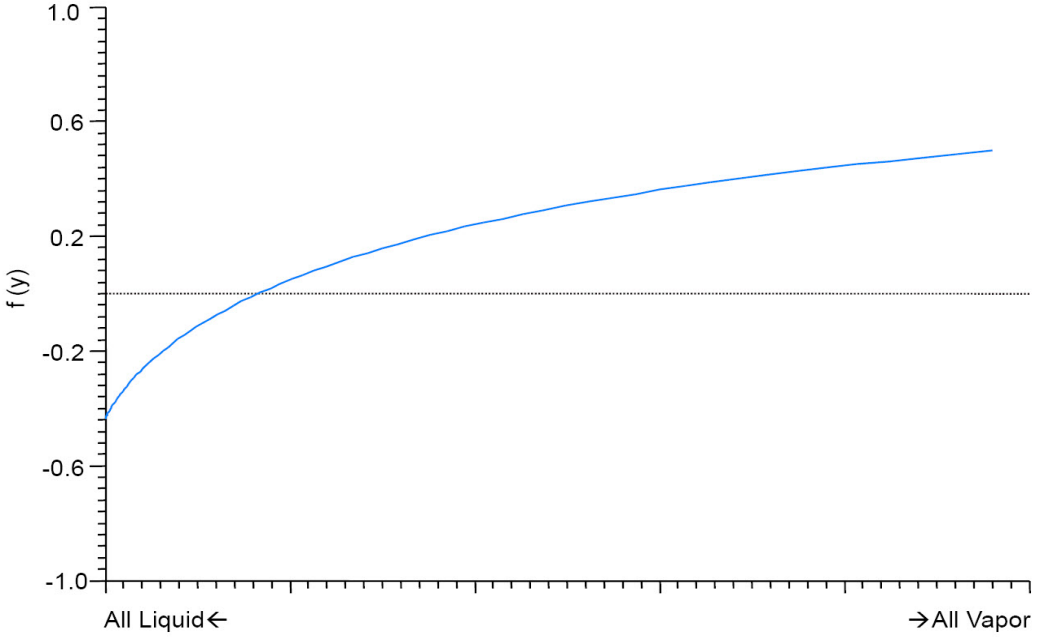

Figure 11: SuperChems Expert Churn turbulent numerical solution of Equation 2 using G_m

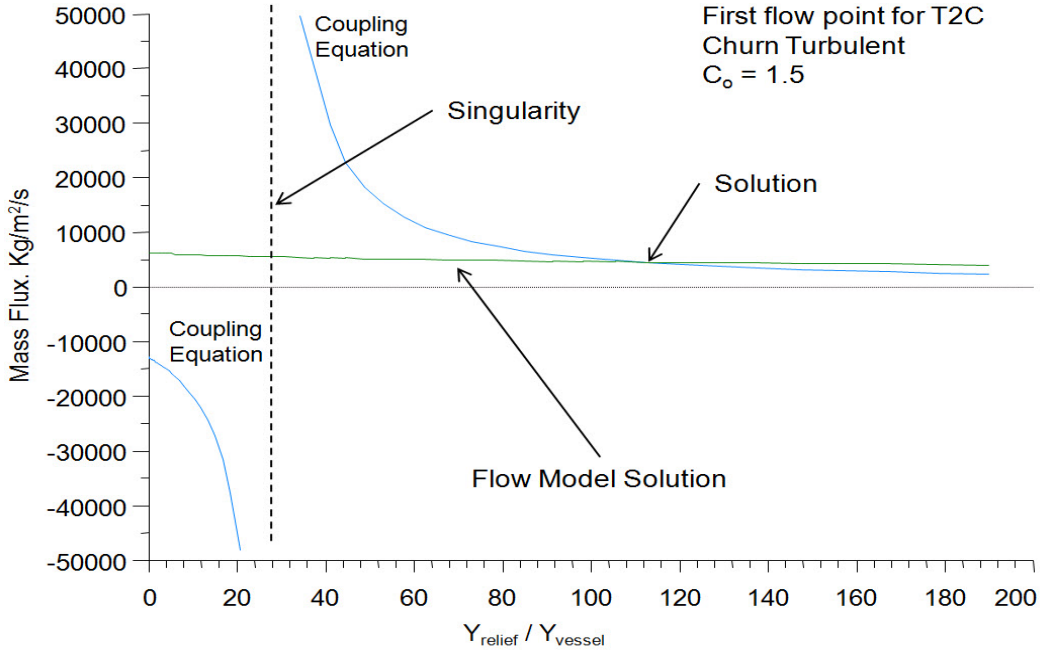

Figure 12: SuperChems Expert Bubbly estimates of pressure for test T12A

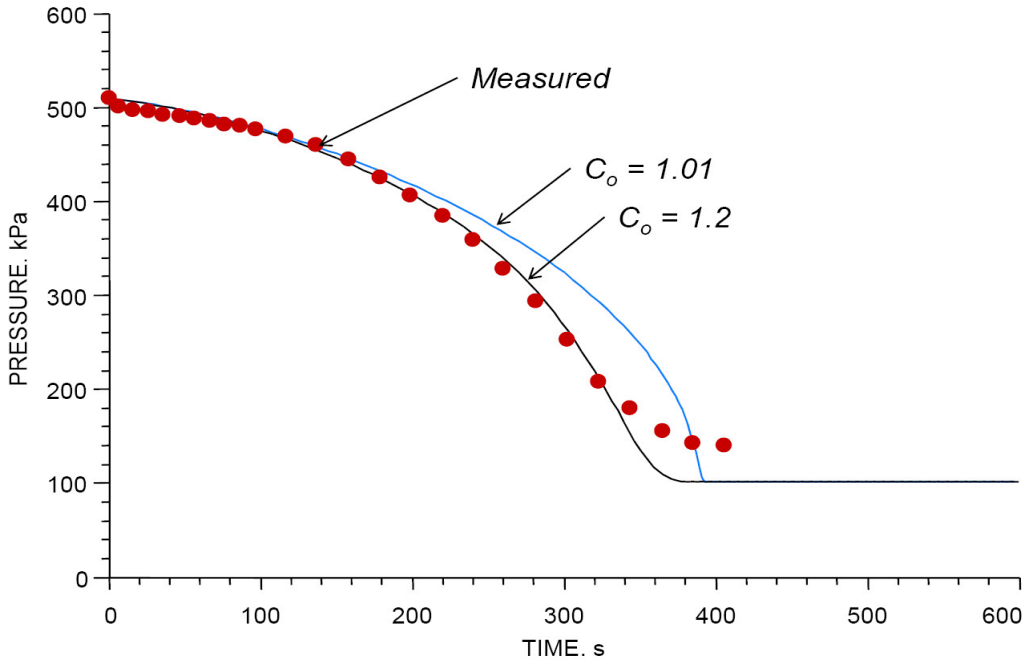

Figure 13: SuperChems Expert Bubbly estimates of vessel void fraction for test T12A

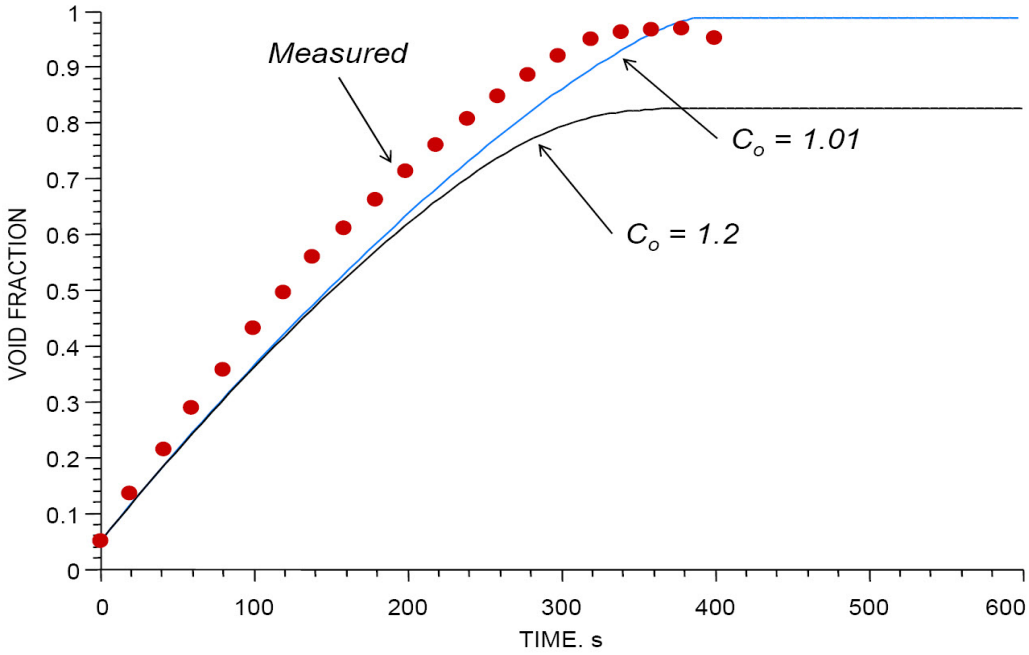

Figure 14: SuperChems Expert Bubbly estimates of vessel mass flow for test T12A

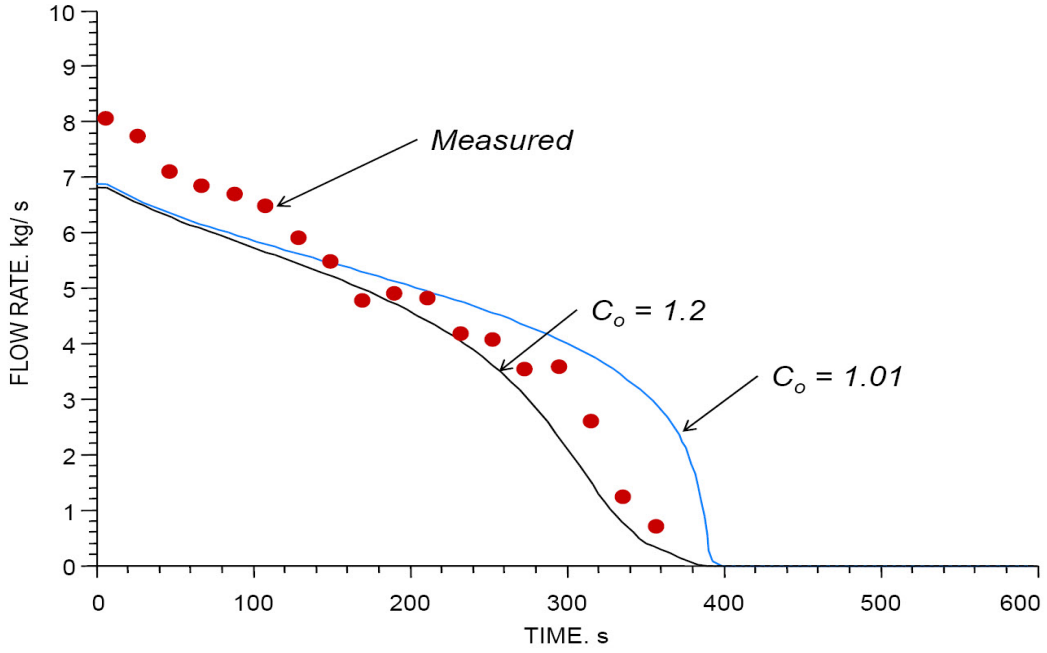

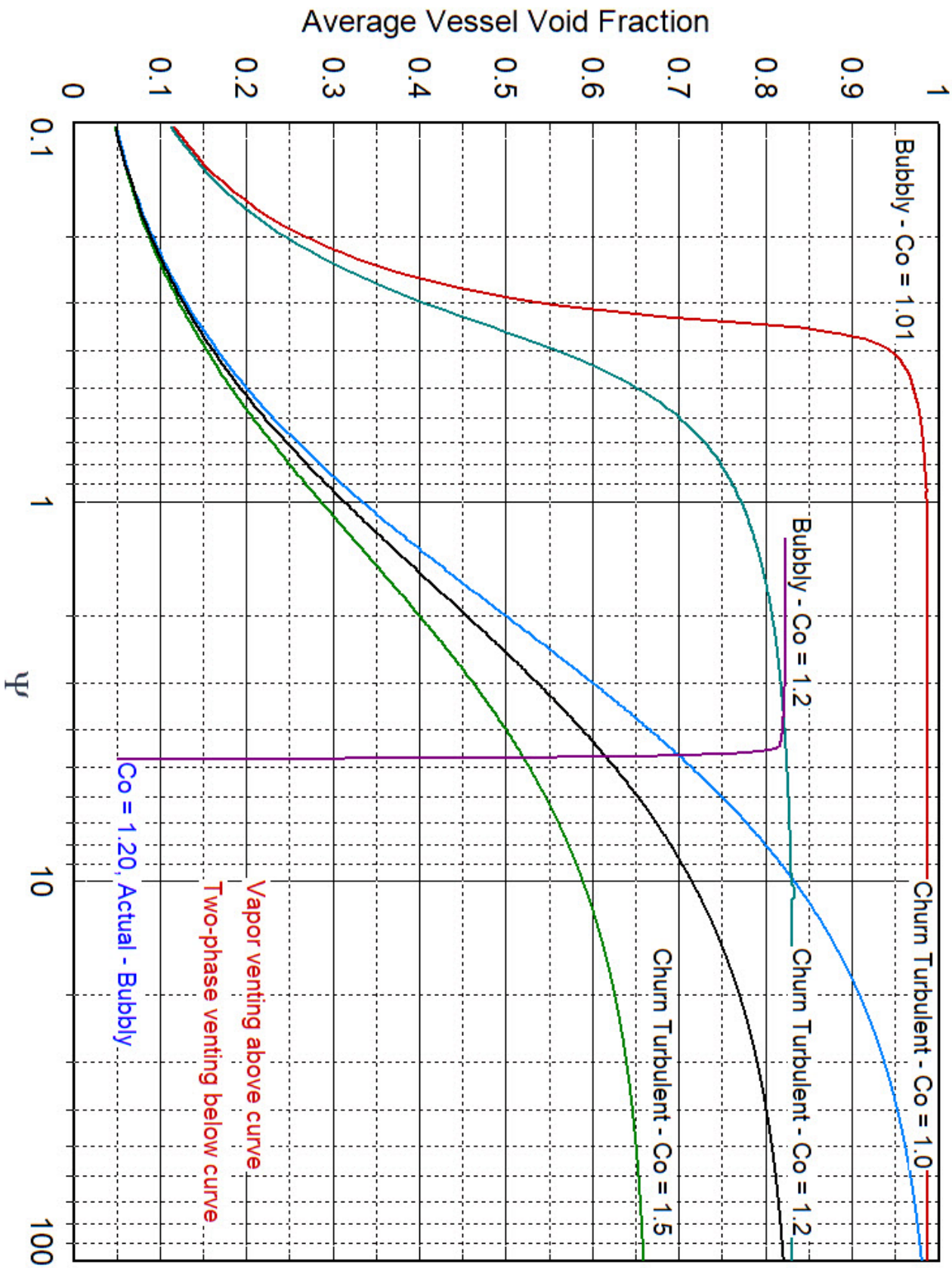

Figure 15: SuperChems Expert Bubbly estimate of α vs. ψ for test T12A

References

[1] M. Grolmes. Foaming systems, fundamentals (part 1). In *Spring DIERS Users Group Meeting, Las Vegas, Nevada*. AIChE, May 2006.

[2] H. K. Fauske and M. Epstein. Source term considerations in connection with chemical accidents and vapor cloud modeling. *Journal of Loss Prevention Process Industries*, 1:75–83, 1988.

[3] Fauske and Associates Inc. Emergency relief systems for runaway chemical reactions and storage vessels: a summary of multiphase flow methods. Technology summary, AIChE/DIERS, 1986.

[4] M. Grolmes and H. Fisher. Vapor liquid onset/disengagement modeling for emergency relief discharge evaluation. In *AIChE Summer National Meeting*, 1994.

[5] G. A. Melhem. Eliminate the DIERS coupling equation singularity. In *DIERS Users Group Meeting*. AIChE, Fall 2008.

[6] M. Levin. Developments in disengagement. In *DIERS Users Group Meeting*. AIChE, Fall 2015.

[7] AIChE/DIERS. Emergency relief systems for runaway chemical reactions and storage vessels: A summary of multiphase flow methods. Technical Report FAI/83-27, Fauske and Associates Inc., 1983.

[8] H. K. Forester and N. Zuber. Growth of a vapor bubble in a superheated liquid. *Journal of Applied Physics*, 25(4):474–478, 1954.

[9] G. B. Wallis. *One-Dimensional Two-Phase Flow*. McGraw-Hill Book Company, New York, 1st edition, 1969.

[10] K. Nakajima, J. W. Palen, and J. Taborek. Analysis and prediction of entrainment and its application to kettle reboiler shell sizing. Technical Report B-K-1/2, Heat Transfer Research, Inc. HTRI, 1970.

[11] H. G. Fisher et al. *Emergency relief system design using DIERS technology. The DIERS project manual.* AIChE/DIERS, 1992.

[12] G. Hendrickson and G. A. Melhem. Fire exposure modeling considerations. *ioMosaic Corporation Publication*, October 2023.

[13] H. G. Fisher and H. S. Forrest. Protection of storage tanks from two-phase flow due to fire exposure. *Process Safety Progress*, 14(3):183–199, July 1995.

[14] H. K. Fauske, M. Epstein, M. Grolmes, and J. Leung. Emergency relief vent sizing for fire emergencies involving liquid-filled atmospheric storage vessels. *Plant/Operations Progress*, 5(4):205–208, 1986.

[15] M. Grolmes and M. Epstein. Vapor-liquid disengagement in atmospheric liquid storage vessels subjected to external heat source. In *19th Annual Loss Prevention Symposium, AIChE Spring National Meeting*, March 1985.

[16] L. L. Simpson. Fire exposure of liquid-filled vessels. *Process Safety Progress*, 20(1):27–32, 2002.

[17] G. E. Scarponia, I. Bradley, G. Landucci, A. M. Birk, and V. Cozzania. Modelling pressure tanks under fire exposure: Past experience, current challenges and future perspectives. *Chemical Engineering Transactions*, 90:481–486, April 2022.

[18] A. M. Birk. Scale effects with fire exposure of pressure-liquefied gas tanks. *Journal of Loss Prevention in the Process Industries*, 8(5):275–290, 1995.

[19] A. M. Birk. Fire testing and computer modelling of rail tank-cars engulfed in fires: Literature review. Technical Report TP 14561E, Transport Canada, March 2006.

[20] Chin-Shun Lin and M. M. Hassan. Numerical investigation of the thermal stratification in cryogenic tanks subjected to wall heat flux. Technical Report NASA Technical Memorandum 103194, NASA, JULY 1990.

[21] G. A. Melhem. Driving safety and business performance through data mining. *ioMosaic Corporation Publication*, 2019.

[22] J. Mishima and D. Pinkston. DOE handbook airborne release fractions/rates and respirable fractions for nonreactor nuclear facilities. Technical Report DOE-HDBK-3010-94, Vol. 1, U.S. Dept. of Energy, Washington, D.C., 1994.

[23] D. F. Paddleford and J. K. Thomas. Waste tank deflagration source generation mechanisms. Technical Report WSRC MS-95-0001, Westinghouse Savannah River Co., Aiken, SC, 1995.

[24] B. E. Hey and D. S. Leach. A model for predicting respirable releases from pressurized leaks. Technical Report WHC-SD-GN-SWD-20007, Westinghouse Hanford Co., Richland, WA, 1994.

[25] D. A. Shaw. Thermodynamic consistency of the DIERS coupling equation. In *DIERS Users Group Meeting*. DIERS, AIChE, October 2000.

[26] S. N. Balasubrahmanyam. Einstein, parachor and molecular volume: Some history and a suggestion. *Current Science*, 94(2):1650–1658, JUNE 2008.

....

Index

About the Authors

Dr. Melhem is an internationally known pressure relief and flare systems, chemical reaction systems, process safety, and risk analysis expert. In this regard he has provided consulting, design services, expert testimony, incident investigation, and incident reconstruction for a large number of clients. Since 1988, he has conducted and participated in numerous studies focused on the risks associated with process industries fixed facilities, facility siting, business interruption, and transportation.

Prior to founding ioMosaic® Corporation, Dr. Melhem was president of Pyxsys Corporation; a technology subsidiary of Arthur D. Little Inc. Prior to Pyxsys and during his twelve years tenure at Arthur D. Little, Dr. Melhem was a vice president of Arthur D. Little and managing director of its Global Safety and Risk Management Practice and Process Safety and Reaction Engineering Laboratories.

Dr. Melhem holds a Ph.D. and an M.S. in Chemical Engineering, as well as a B.S. in Chemical Engineering with a minor in Industrial Engineering, all from Northeastern University. In addition, he has completed executive training in the areas of Finance and Strategic Sales Management at the Harvard Business School. Dr. Melhem is a Fellow of the American Institute of Chemical Engineers (AIChE) and Vice Chair of the AIChE Design Institute for Emergency Relief Systems (DiERS).

Contact Information

Georges. A. Melhem, Ph.D., FAIChE
E-mail. melhem@iomosaic.com

ioMosaic Corporation
93 Stiles Road
Salem, New Hampshire 03079
Tel. 603.893.7009, x 1001
Fax. 603.251.8384
web. www.iomosaic.com

How can we help?

Please visit www.iomosaic.com and www.iokinetic.com to preview numerous publications on process safety management, chemical reactivity and dust hazards characterization, safety moments, video papers, software solutions, and online training.

In addition to our deep experience in process safety management (PSM), chemical reaction systems, and the conduct of large-scale site wide relief systems evaluations by both static and dynamic methods, we understand the many non-technical and subtle aspects of regulatory compliance and legal requirements. When you work with ioMosaic® you have a trusted ISO certified partner that you can rely on for assistance and support with the lifecycle costs of relief systems to achieve optimal risk reduction and PSM compliance that you can evergreen. We invite you to connect the dots with ioMosaic®.

We also offer laboratory testing services through ioKinetic® for the characterization of chemical reactivity and dust/flammability hazards. ioKinetic® is an ISO accredited, ultramodern testing facility that can assist in minimizing operational risks. Our experienced professionals will help you define what you need, conduct the testing, interpret the data, and conduct detailed analysis. All with the goal of helping you identify your hazards, define and control your risk.

ioMosaic®
Minimizing risk. Maximizing potential.®

About ioMosaic Corporation

Our mission is to help you protect your people, plant, stakeholder value, and our planet.

Through innovation and dedication to continual improvement, ioMosaic has become a leading provider of integrated process safety and risk management solutions. ioMosaic has expertise in a wide variety of disciplines, including pressure relief systems design, process safety management, expert litigation support, laboratory services, training, and software development.

As a certified ISO 9001:2015 Quality Management System (QMS) company, ioMosaic offers integrated process safety and risk management services to help you manage and reduce episodic risk. Because when safety, efficiency, and compliance are improved, you can sleep better at night. Our extensive expertise allows us the flexibility, resources, and capabilities to determine what you need to reduce and manage episodic risk, maintain compliance, and prevent injuries and catastrophic incidents.

Consulting Services

- Asset Integrity
- Auditing
- Due Diligence
- Facility Siting
- Fault Tree/SIL Analysis
- Fire & Explosion Dynamics
- Incident Investigation, Litigation Support, and Expert Testimony
- Hydrogen Safety
- LNG Safety
- LPG Safety
- Pipeline Safety
- Process Hazard Analysis
- Process Engineering Design and Support
- Process Safety Management
- Relief and Flare Systems Design and Evaluation
- Risk Management Program Development
- Quantitative Risk Assessment
- Software Solutions
- Structural Dynamics
- Sustainability Reporting Support
- Technology Transfer Package Development
- Process Safety Training

Laboratory Testing Services (ISO Accredited)

- Battery Safety Testing
- Chemical Reactivity Testing
- Combustible Dust Hazard Analysis and Testing
- Flammability Testing
- Physical Properties Testing
- Process Safety Services
- Specialized Testing

US Offices

Salem, New Hampshire
Houston, Texas
Minneapolis, Minnesota
Berkeley, California

International Offices

Al Seef, Kingdom of Bahrain
Bath, United Kingdom

Software Solutions

Process Safety Office®: A suite of integrated tools for process safety professionals and risk analysts.

Process Safety Enterprise®: Process Safety Management compliance made easy with enterprise workflows, dynamic forms, document management, key performance indicators and metrics, and more.

Process Safety Learning®: Build your process safety competencies incrementally using learning modules.

Process Safety tv®: The worldś first video streaming platform dedicated to process safety.

Contact us

www.ioMosaic.com
sales@ioMosaic.com
1.844.ioMosaic